

Lift Generation Due to Vortex Shedding

By

Koichi OSHIMA and Yuko OSHIMA*

(February 1, 1983)

1. Impulsively Started Airfoil

It is said that, in incompressible, invicid uniform flow, two-dimensional airfoil generates lifting force due to its bound vortex (Joukowski's theorem), and that the starting vortex left behind the impulsively started airfoil has the same strength to this bound vortex with opposite sign, then Kelvin's circulation theorem is not violated [1]. This statement has been confirmed experimentally, and the lift force thus generated is expressed as $\rho U \Gamma$, where ρ is the flow density, U is the flow velocity and Γ is the bound circulation. In Fig. 1, the flow field around an impulsively started airfoil is schematically illustrated, in which the positions of the particles originally placed on the line perpendicular to the moving direction at the leading edge are shown at several time instants after the impulsive start. These lines are considered as the equi-potential lines at each time instant and the discontinuities along the airfoil surface and on the wake centerline are mentioned.

The Bernoulli equation taken along the stream line just above the airfoil surface is written as

$$\frac{\partial \phi_1}{\partial t} + \frac{1}{2} u_1^2 + \frac{p_1}{\rho} = \text{const.}$$

where ϕ_1 is the potential, u is the local flow velocity, ρ is the density which is a constant, p is the pressure and the suffix 1 denotes the stream line along the upper surface. Similarly, the one along the lower surface is written as

$$\frac{\partial \phi_2}{\partial t} + \frac{1}{2} u_2^2 + \frac{p_2}{\rho} = \text{const.}$$

where the suffix 2 denotes the lower surface stream line. These constant values must be same since they started at the same upstream position. The values of the surface pressure should be unique everywhere on the surface, including at the trailing edge, therefore $p_1 = p_2$, which is a form of the Kutta-Joukowski condition. Taking the difference of these equations, one obtains

$$\frac{\partial}{\partial t} (\phi_1 - \phi_2) = -\gamma U$$

* Dept. Physics, Ochanomizu University

where $U = \frac{1}{2}(u_1 + u_2)$ and $\gamma = u_1 - u_2$ is the vorticity created at the trailing edge per unit time. This means that the bound vortex strength is equal to the vorticity flowing out at the trailing edge with the mean velocity. In this way, the flowing out vorticity does contribute to the lift generation.

This situation is more clearly demonstrated by numerical simulation using discrete vortex method [2]. Figure 2 shows the flow pattern around the impulsively

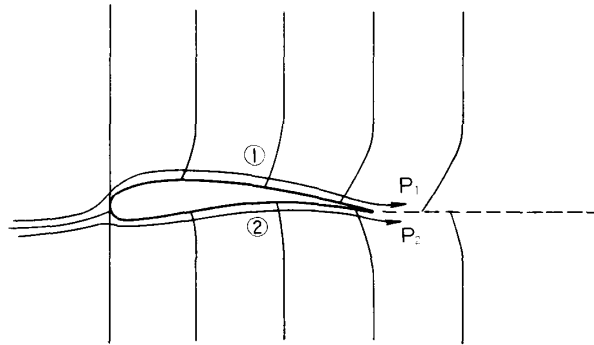


Fig. 1. Particle traces placed originally along the vertical line at the leading edge. Each line shows successive trace after impulsive start.

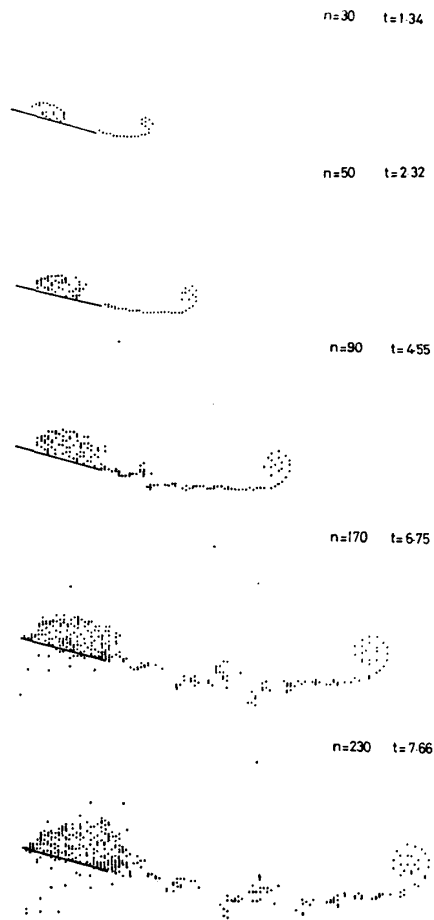


Fig. 2. Discrete vortex simulation of the flow around an impulsively started flat plate at successive time instants.

started flat plate with an angle of incidence, in which the discrete vortices are shed at both the leading and trailing edges and their positions are plotted. It is seen, that the vortices shed at the leading edge are trapped around the upper surface of the airfoil and do not contribute to the lift generation. On the other hand, those generated at the trailing edge immediately flow down and create the lift force.

2. Lift Generation by Stationary Trapped Vortex

The lift force of an airfoil can be enhanced by placing an organized vortex in the vicinity of the wing. A well-known example is the additional lift produced by the vortex sheets rolling up along the leading edge of a delta wing flying at large angles of attack. Also Kasper suggested that spanwise vortices could be generated and maintained on the upper surface of a wing by deploying specially designed flaps and extremely high lift coefficients could be realized [3]. Saffman and Sheffield [4] made an analysis of a flat-plate airfoil with an attached vortex and showed that at suitable locations a line vortex might become stationary relative to the airfoil. That is, the vortex is stable to small disturbances at some of the equilibrium locations, and according to their theoretical investigation, the vortex-augmented lift was significant.

The schematic in Fig. 3 explains how an external vortex can increase the lift on an airfoil. For an airfoil without attached vortices, in order to satisfy the Kutta-Joukowski condition at the sharp trailing edge, a circulation Γ is created around the airfoil, which gives the lift of $\rho U \Gamma$ per unit span of the airfoil. When a vortex with the strength Γ' is placed above the airfoil, it induces a reversed fluid motion on the upper surface, so that infinite velocity would appear at the trailing edge. In order to avoid this, additional circulation $-\Gamma'$ has to be generated at the trailing edge and flows down into the wake, so that the strength of the bound vortex increases by Γ' and the Kutta-Joukowski condition is fulfilled again. Another words, a vortex circulation $-\Gamma'$ is shed in the wake and the airfoil has thus gained a lift of $\rho U (\Gamma + \Gamma')$ per unit span.

M.-K. Huang and C.-Y. Chow [5] showed that, although very high lifting force can be generated by a stationary vortex captured above the leading edge, this vortex is always unstable. The maximum lift that can be generated by a stable vortex trapped above the trailing edge is generally several times higher than the

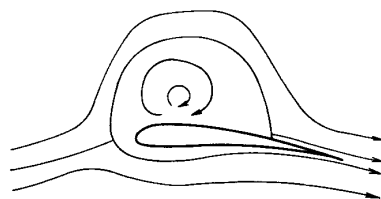


Fig. 3. Schematic flow pattern around an airfoil with a vortex trapped on the upper surface.

lift on the same airfoil without an external vortex. They have also discussed on the effects of the airfoil thickness, camber and the angle of attack. In later paper [6], they traced the movement of a vortex placed on an airfoil and found the airfoil lift and moment coefficients as well as the surface pressure distributions. The results confirmed the above-stated lift generation mechanism.

3. The Weis-Fogh Circulation-Generation Mechanism

Weis-Fogh [7] described a model of insect flight which suggested a new mechanism for generating circulation (Fig. 4). This consists of the opening operation of a V-shaped wing segment and the subsequent separation of the two segments. During the opening phase, equal and opposite circulation around each segment is created without violating Kelvin's theorem and without shedding vortices, and subsequently a lift from this circulation is generated when the wings are parted. Lighthill [8] presented a two-dimensional inviscid analysis of this opening phase, including the effect of a leading edge separation bubble. The latter was concluded to give a rather weak effect on the induced circulation. Later experiments by Maxworthy [9], however, showed substantial effect of the leading edge separation.

Recently, R. H. Edwards and H. K. Cheng [10] analysed this problem and showed that the vortex shedding has an important influence on the flow field. As the results of the separation, the circulation on each member of the wing pair is significantly augmented over most of the range of the opening angle, thus greatly enhancing the Joukowski lift as perceived originally by Weis-Fogh. The growth rate of the vortex strength as well as the vortex center movement predicted by their analysis are found to be consistent with the laboratory data by Maxworthy.

The success of Weis-Fogh's clap-fling mechanism depends on the circulation achieved by each wing at the end of the opening phase and the subsequent shedding of it during the separation phase. This circulation created during the opening phase, which is not determined by the initial Joukowski lift alone, may play a significant role. Since the aerodynamic forces acting on the flapping wing is induced by the circulation which flows down apart, it is suggested that this unsteady trapped separation vortex contributes to them.

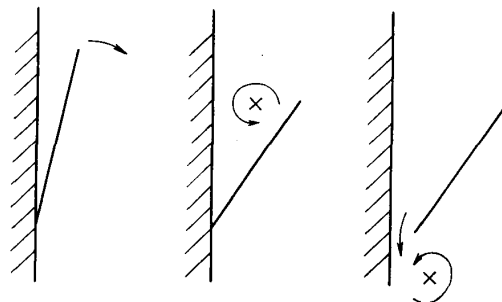


Fig. 4. Two-dimensional Weis-Fogh lift generation mechanism. Only the half portion of the symmetrical configuration is shown.

4. Autorotation of Symmetrical Airfoil

Some two-dimensional, symmetrical bodies such as flat plates or elliptic cylinders, the axis of which is set perpendicularly to the oncoming uniform flow, can sustain autorotation, when a sufficiently strong initial drive is applied in order that the

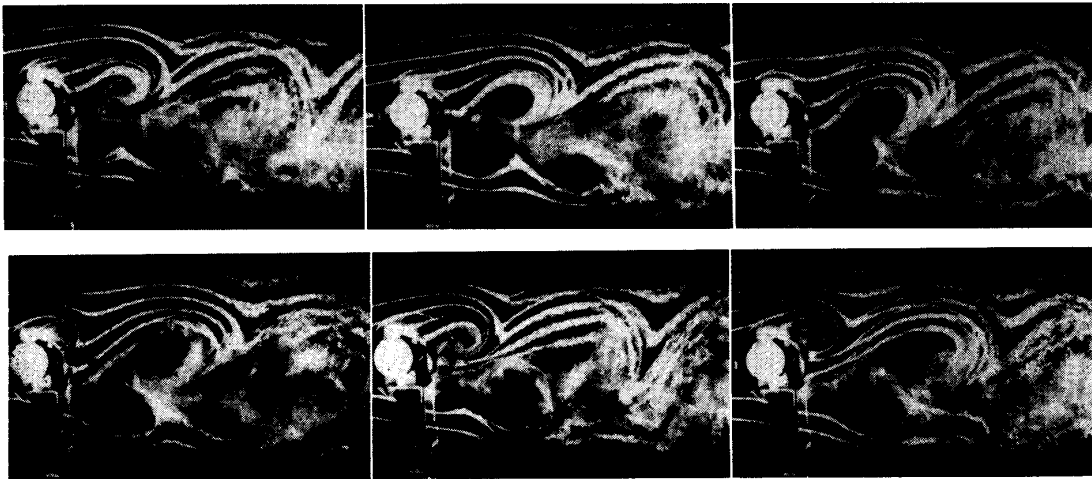


Fig. 5. Flow fields around an autorotating elliptic airfoil visualized by smoke wire method. The field was illuminated by multi-flashed strobo-light synchronized with the autorotation phase. The pictures were taken at each 30 degree phase angle.

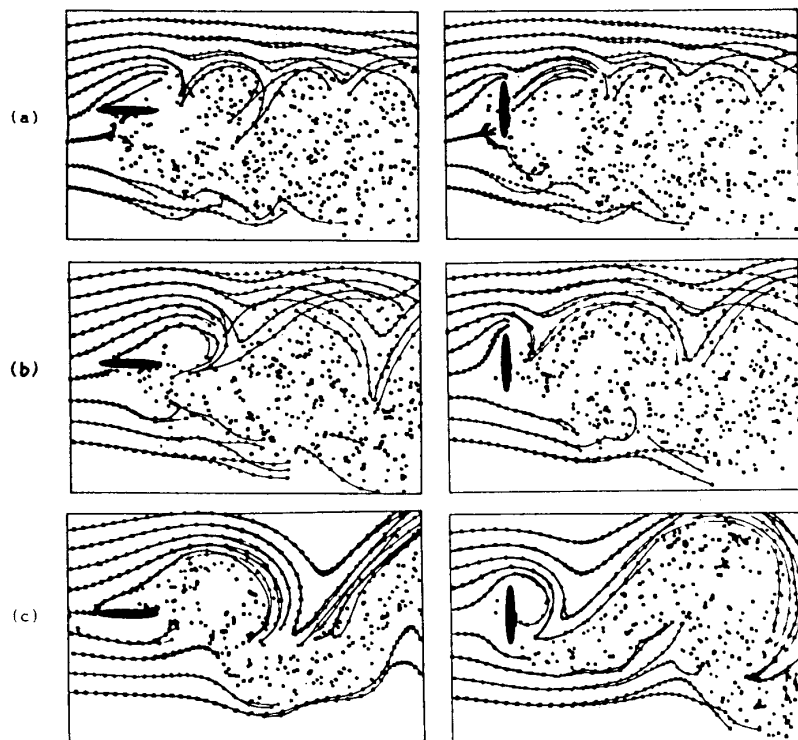


Fig. 6. Numerically simulated streak lines at phase angles of 0 and 90 degrees. The pairs of two from top to bottom correspond to the Strouhal number of 0.4, 0.2 and 0.1, respectively.

flow initiates continuous rotation of the body. This type of autorotation has been extensively investigated by E. H. Smith, etc. [11]–[15].

The flow patterns around an autorotating elliptic airfoil are shown in Fig. 5, in which the instantaneous streak lines were visualized by smoke wire method. Figure 6 shows those simulated numerically, in which the airfoil is driven externally at the specified Strouhal numbers. The rotating angular velocity was

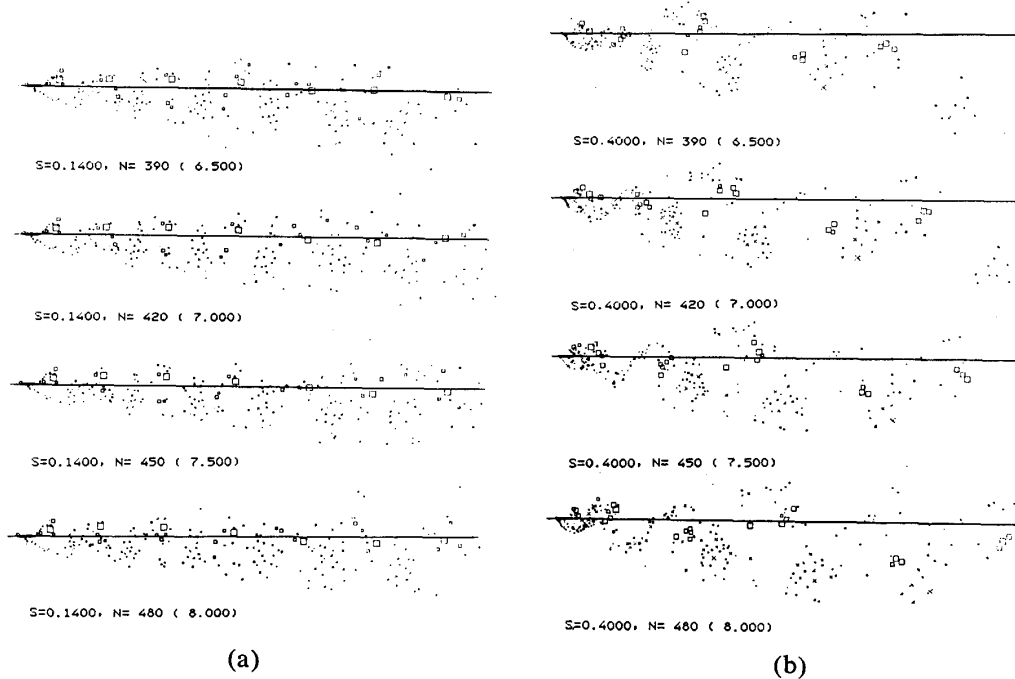


Fig. 7. Numerically simulated vortex distributions along the wake with the Strouhal numbers of 0.14 as (a) and 0.4 as (b). The patterns correspond to each half cycle of rotation.

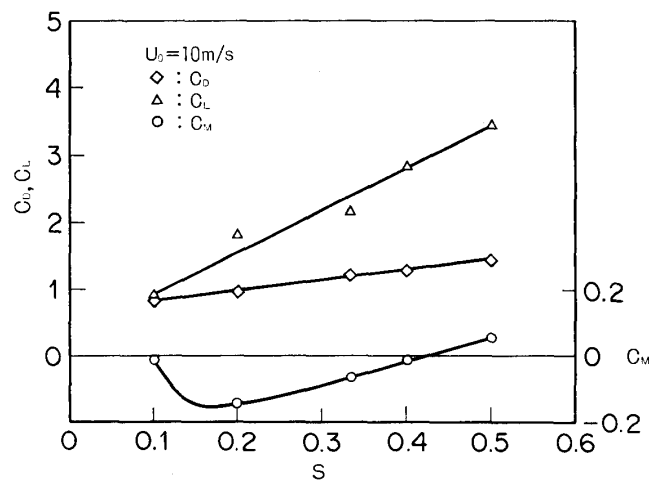


Fig. 8. Aerodynamic forces predicted by numerical simulation. C_D , C_L and C_M correspond to the lift, drag and moment coefficients, respectively. S is the Strouhal number of the rotation which was assumed to be constant.

varied over a wide range which includes the autorotation condition. As seen in these pattern, a large vortex is created behind the leading edge during the receding phase of the leading edge, which is trapped for a while on the downstream side of the airfoil and eventually flows downstream during the progressing phase of the leading edge. Although other smaller vortices are observed around the trailing edge also, they vary their shape and number depending upon the rotating frequency and are unstationary. Contrary that, this large trapped vortex is quite stable. Therefore, aerodynamic forces on the rotating airfoil may strongly influenced by this trapped vortex.

The numerically simulated wake pattern is shown in Fig. 7, in which the vortex distributions in the wake of the rotating airfoil with the Strouhal number of 0.14 and 0.4 are plotted at the same succeeding phase angles. For the flow with the Strouhal number of 0.14, the wake oscillation and the airfoil rotation are coherent, but the case of 0.4 shows that they have different frequency. That is, the

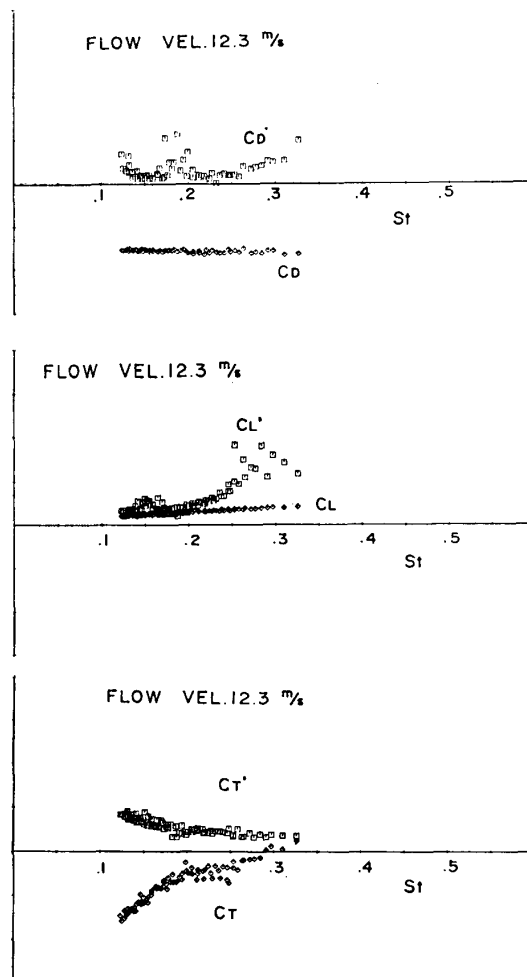


Fig. 9. Aerodynamic forces measured by wind tunnel experiment. C_D , C_L and C_T correspond to the drag, lift and torque coefficients, respectively, and the primes denote the root mean square deviation over one cycle of rotation. St is the Strouhal numbers of the forced rotation.

shedding of the large trapped vortex is not resonance with the airfoil rotation. Figure 8 gives the aerodynamic forces obtained by the numerical simulation, in which the coherent condition of airfoil rotation and the wake oscillation coincides with the minimum torque condition of the airfoil (maximum rotation-driving torque), and increase of the discrepancy between them decreases the driving force and eventually acts as retarding force of rotation. This feature is also confirmed by the measured values of the aerodynamic force coefficients shown in Fig. 9.

5. Concluding Remarks

The stationarily trapped vortex in the vicinity of an airfoil induces lifting force according to the Joukowski theorem, and the induced bound circulation is determined using the Kutta condition and Kelvin's circulation theorem. The moving vortex near an airfoil may also produce lift owing to the induced bound circulation. Its strength is determined by the part of the vortex strength which is supposed to be stationary. That is: Suppose that the strength of the free vortex is divided into two parts, the one is flowing with the uniform flow velocity and the other is stationary relative to the airfoil. Then the latter contributes to the lift generation, but the former does not.

References

- [1] Imai, I: Fluid Mechanics Part I, Shookabo Pub. (1978) (in Japanese).
- [2] Oshima, Y and Oshima, K: Vortical Flow Behind an Oscillating Airfoil, 15 ICTAM Toronto, ed. F. P, J. Rimrott etc. p. 357-368 (1981).
- [3] Cox, J: The Revolutionary Kasper Wing, Soaring Vol. 37, pp. 20-23 (1973)
- [4] Saffman, P. G. and Sheffield, J. S.: Flow over a Wing with an Attached Free Vortex, Studies in Appl. Math. Vol. 57, pp. 107-111 (1977).
- [5] Huang, M.-K. and Chow, C.-Y.: Trapping of a Free Vortex by Joukowski Airfoil, AIAA J Vol. 20, p, 292-298 (1982).
- [6] Chow, C.-Y. and Huang, M.-K.: Unsteady Flows About a Joukowski Airfoil in the Presence of Moving Vortices, AIAA Paper 83-0129.
- [7] Weis-Fogh, T: Quick Estimates of Flight Fitness in Hovering Animals, Including Novel Mechanism for Lift Production, J. Exp. Biol. Vol. 59, p. 169-230 (1973).
- [8] Lighthill, M. J.: *Mathematical Biofluidynamics*, SIAM (1975).
- [9] Maxworthy, T.: Experiments on the Weis-Fogh Mechanism of Lift Generation by Insects in Hovering Flight. Part I. Dynamics of the "Fling", JFM. Vol. 93, p. 47-64, (1979).
- [10] Edwards, R. H. and Cheng, H. K.: The Separation Vortex in the Weis-Fogh Circulation-Generation Mechanism, JFM Vol. 120, p. 463-473 (1982).
- [11] Smith, E. H.: Autorotating Wings: and Experimental Investigation, JFM Vol. 50, p. 513-534 (1971).
- [12] Iversen, J. D.: Autorotating Wings: the Effect of the Moment of Inertia, Geometry and Reynolds Number, JFM Vol. 92, pp. 327-348 (1979).
- [13] Lugt, H. J. and Ohring, S.: Rotating Elliptic Cylinder in a Viscous Fluid at Rest or in a Parallel Stream, JFM Vol. 73, pp. 127-156 (1977).
- [14] Lugt, H. J.: Autorotation of an Elliptic Cylinder about an Axis Perpendicular to the Flow, JFM Vol. 99, pp. 817-840 (1979).
- [15] Oshima, Y., Izutsu, N., Oshima, K. and Kuwahara, K.: Autorotation of an Elliptic Airfoil, AIAA Paper 83-0130 (1983).